14th Annual (International) Mechanical Engineering Conference – May 2006
Isfahan University of Technology, Isfahan, Iran

COMPUTATIONAL FLOW SEPARATION CONTROL USING ELECTROMAGNETIC FIELDS

S. A. Akbari[1], A. Sedaghat[2] and A. R. Azimian[3]
Department of Mechanical Engineering
Isfahan University of Technology, Isfahan, Iran
E-mail: Sedaghat@cc.iut.ac.ir

Abstract
Flow separation control by electromagnetic field was studied for a flat plate at high angles of incidence. Lorentz force was used as the model for the electromagnetic field and incorporated within a compressible Navier-Stokes flow solver. The compressible solver is based on an implicit, high resolution, and Total Variation Diminishing (TVD) scheme. The computational results were qualitatively compared with experimental observations. For a range of incidence angles, the electromagnetic field has completely prohibited flow separation and enhanced lift coefficient. However, the overall drag coefficient has been slightly increased due to the increase in skin friction.

Keywords: Electromagnetic Field – Lorentz Force – Flow Separation – Navier-Stokes – TVD Schemes.

Introduction
Control of flow separation by suction was first demonstrated by Ludwig Prandtl [1] together with the presentation of his boundary layer theory. Since that time, many active and passive techniques to control wall bounded flows have been developed. If the fluid is electrically conducting, an additional possibility of flow control is given by the application of a Lorentz force f. This electromagnetic body force results from the vector product of the magnetic induction B and the current density j.

$$f = j \times B \tag{1}$$

The current density is given by ohm's law

$$j = \sigma(E + U \times B) \tag{2}$$

E denotes the electric field, U the velocity, and σ is the electrical conductivity, respectively.

Depending on the conductivity of the fluid, one can distinguish between two different types of magneto hydrodynamic (MHD) flow control. If the fluid has a high conductivity in the order of $\sigma \approx 10\, S/m$ like liquid metals or semiconductor melts, an external applied magnetic field alone can have a strong influence on the flow. As described in the second term in the right hand side of Equation 2, the interaction of the flow with the magnetic field causes electrical currents in the liquid. These currents again interact with the external field and generate the Lorentz force field as given by Equation 1. Typical electrolytes like seawater possess a much lower electrical conductivity in the order of $\sigma \approx 10\, S/m$. Therefore, electrical current generated by the $U \times B$ term are too small to produce a noticeable Lorentz force. In order to obtain current densities large enough for flow control purposed in electrolytes, an additional external electric field E has to be applied.

The idea to influence the boundary layer of a low conducting fluid by electromagnetic force dates back to the 1960s [2]. Only recently, it has attracted new attention to control turbulent boundary layers [3-6]. Several different force configurations have been investigated mainly with the aim to reduce the skin friction of turbulent boundary layers.

The application of wall normal Lorentz force has been studied experimentally by Nosenchuck and Coworkers [3,7] which suggest strong reduction in turbulent skin friction. However, numerical simulations of comparable configuration by O'Sullivan and Bitingen [8] and Crawford have not shown this strong reduction.

[1] Postgraduate Student (sayedaliakbari@yahoo.ca)
[2] Assistant Professor
[3] Associate Professor

The use of wall parallel forces in streamwise direction to control separation occurrence was first proposed by Lielausis and Gailitis [2]. The influence of such a force on a turbulent boundary layer has been studied experimentally by Henoch and stace [5] and numerically by Crawford and Karniadakis [6]. Both report a reduction of stream wise velocity fluctuations, but also an increase of the skin friction with applied Lorentz force.

The aim of the present article is to investigate boundary layer separation control for compressible flows. A high-resolution, implicit, and TVD solver was used to solve compressible Navier-Stokes equations. The investigations are focused on the use of wall parallel Lorentz forces in streamwise direction to control a separated boundary layer flow over a flat plate at high angles of incidence.

2 Governing Fluid Flow Equations

Neglecting body forces and volumetric heating, the non-dimensional form of compressible Navier-Stokes equations in the transformed coordinate system for two dimensional flows can be written as:

$$\frac{\partial \hat{U}}{\partial t}+\frac{\partial \hat{F}}{\partial \xi}+\frac{\partial \hat{G}}{\partial \eta}=0 \tag{3}$$

where

$$\hat{U}=U/J$$

$$\hat{F}=(\xi_x F+\xi_y G)/J\ ,\ \hat{G}=(\eta_x F+\eta_y G)/J \tag{4}$$

$$J=\xi_x\eta_y-\xi_y\eta_x$$

$\xi=\xi(x,y)$, $\eta=\eta(x,y)$ are coordinate transformation function and J is the Jacobian of the transformation. The vectors U , F and G are given by:

$$U=\begin{bmatrix}\rho\\ \rho u\\ \rho v\\ e\end{bmatrix}\ ,\ F=\begin{bmatrix}\rho u\\ P+\rho u^2-\tau_{xx}\\ \rho uv-\tau_{xy}\\ (e+P)u-u\tau_{xx}-v\tau_{xy}+q_x\end{bmatrix},$$

$$G=\begin{bmatrix}\rho v\\ \rho uv-\tau_{xy}\\ P+\rho v^2-\tau_{yy}\\ (e+P)v-u\tau_{xy}-v\tau_{yy}+q_y\end{bmatrix} \tag{5}$$

where ρ , u , v , e , q are respectively density, velocity components along x, y directions, total energy and heat flux. The components of shear stress tensor are as follow:

$$\tau_{xx}=\frac{\mu}{\mathrm{Re}}\left(\frac{4}{3}\frac{\partial u}{\partial x}-\frac{2}{3}\frac{\partial v}{\partial y}\right)$$

$$\tau_{yy}=\frac{\mu}{\mathrm{Re}}\left(\frac{4}{3}\frac{\partial v}{\partial y}-\frac{2}{3}\frac{\partial u}{\partial x}\right) \tag{6}$$

$$\tau_{xy}=\frac{\mu}{\mathrm{Re}}\left(\frac{\partial u}{\partial y}+\frac{\partial v}{\partial x}\right)$$

The governing Navier-Stokes equations have been used in non-dimensional form.

3 The Electromagnetic Force

The concept of a streamwise Lorentz force was first proposed by Gailitis and Lielausis [2] to stabilize a laminar flat plate boundary layer. The force distribution produced by the stripwise geometry shown in Figure 1 can be calculated by series expansions of the magnetic and electric fields (Grienberg [9]). The resulting force decays in a good approximation exponentially with the wall distance y. Considering also higher terms, a variation of the force density with the spanwise coordinate z appears. This variation arises from the singularities of the equations for the magnetic and electric field at the front of the magnets and electrodes, respectively.

The streamwise Lorentz force can be generated by a strip wise arrangement of electrodes and permanent magnets of alternating polarity and magnetization, respectively; as sketched in Figure 1. If both electric and magnetic fields have only components in y and z direction and neglects the induced currents $\sigma(U\times B)$ compared to the applied one σE , the cross product $j\times B$ has an x component only.

For given magnet configuration the distribution and the amplitude of the force can be determined by the polarity of the electrodes and the magnitude of the current density. That means also time dependent forces can easily be applied by just feeding an appropriate current to the electrodes. However, electrochemical aspects like the production of electrolytic bubbles have to be considered.

In Figure 2 the distribution of the Lorentz force calculated by the finite element Maxwell solver OPERA is shown [10]. An exponential decay away from the wall, but also the distinct maxima of the force caused by the singularities is clearly visible. Averaged over the spanwise coordinate z, the mean force density is given by

$$F=\frac{\pi}{8}j_0 M_0 e^{-\frac{\pi}{a}y} \tag{7}$$

M_0 denotes the magnetization of the magnets and j_0 the applied current density σE_0, respectively. The magnetic induction B_0 at the surface of the magnetic poles can be calculated from the geometry of the magnets and their magnetization M_0. Electrodes and magnets have the same width *a*.

Tsinober and Shtem [11] have used incompressible boundary layer equations to include the electromagnetic force where a non-dimensional parameter is introduced as

$$Z = \frac{\pi}{8} \frac{j_0 M_0 a^2}{\rho U_0 \nu} \tag{8}$$

which describes the ratio of electromagnetic to viscous forces. It corresponds to the square of the Hartmann number if one compares it with usual MHD flows. However, the normalization of the full Navier-Stokes equations leads to an additional non-dimensional parameter

$$N = \frac{j_0 B_0 L}{\rho U_0^2} \tag{9}$$

N is the so-called interaction parameter giving the ratio of electromagnetic to inertial forces. B_0 is the surface magnetization of the permanent magnets and L is a characteristic length equal to the chord length c in the case of hydrofoils. Obviously N, Z and Re are not independent, since Z /N~ Re.

In this study the G flux in the compressible flow equations (3) may be modified as follows

$$G = \begin{bmatrix} \rho v \\ \rho uv - \tau_{xy} + \dfrac{J_0 B_0 a}{\pi \rho U_0^2} \exp\left(\dfrac{-\pi y L}{a}\right) \\ P + \rho v^2 - \tau_{yy} \\ (e+P)v - u\tau_{xy} - v\tau_{yy} + q_y \end{bmatrix} \tag{10}$$

with the free stream velocity of U_0. This allows no further treatment of the numerical algorithm used for solving the full Navier-Stokes equations and can be easily employed for high speeds where shock induced separation may be sought to be controlled.

For the canonical case of a flat Plate boundary layer, the streamwise pressure gradient is zero. Provided Z = 1, the boundary layer thickness reaches an asymptotic value. That means, the momentum loss due to the wall friction is just balanced by the momentum gain caused by the electromagnetic force. This consequences an exponential boundary layer profile of the following type:

$$\frac{u}{U_0} = 1 - e^{\frac{-\pi}{a} y} \tag{11}$$

This profile has two orders of magnitude higher critical Reynolds number than the Blasius profile [12], so that transition will be delayed considerably.

Flow separation occurs according to Prandtl [1] when fluid decelerated by friction forces is exposed to an adverse pressure gradient stronger than the remaining kinetic energy of the fluid. The boundary layer separates from the wall and a recirculation region forms. Consequently, form drag increases and lift possibly decreases.

To prevent separation, the momentum deficit of the boundary layer has to be overcome and the pressure gradient of the outer flow has to be balanced. Experimental demonstration of separation prevention [10] on a flat plate by means of a streamwise Lorentz force has shown in Figure 3.

In Figure 3a, the flow around the plate without Lorentz force at an angle of attack of 18 degrees is shown. Since the Reynolds number based on the plate length is small, i.e. $\mathrm{Re} = 1.2 \times 10^4$, the flow separates laminar at the leading edge without reattachment. Because of the leading edge separation, the flow should be influenced already at the nose of the plate. Consequently, the magnet/electrode array is placed just behind the half cylinder forming the leading edge of the plate.

The flow situation under the influence of a Lorentz force of N = 6.87 [10] is shown in Figure 3b. As the bubble strips indicate, the boundary layer is attached over the whole length of the plate. Due to the pressure rise in the outer flow, the boundary layer fluid is strongly decelerated at the leading edge. By the Lorentz force, the near wall fluid is subjected to acceleration while passing the plate. This can be seen by looking at the shape of the hydrogen bubble stripes near the plate.

Separation of flow causes a form or pressure drag on the moving body simply due to the pressure difference between forward and backward stagnation point. This form drag estimates practically the total drag of bluff bodies at higher Reynolds numbers. Separation prevention can reduce the form drag to zero.

The application of a streamwise Lorentz force for separation prevention has two additional consequences on the drag. On one hand due to the exponential force distribution, the velocity gradient at the wall and therefore wall friction is increased. On the other hand, the force exerts thrust on the body. At high enough forcing parameters a configuration is possible, where thrust overcomes drag.

3 Numerical Method

A class of implicit, second order accurate, total variation diminishing (TVD) scheme has been adopted here for computation of two dimensional compressible flows. The method is based on upwind and symmetric TVD schemes reported by Yee [13] and further modified by Sedaghat [14, 15] for computation of viscous flows. In this work, the symmetric TVD method with the Minmod limiter function was selected due to better predictability for low subsonic flows.

For computation of 2D compressible flows over a flat plate at high incidence angles as sketched in Figure 4, an algebraic grid generator with clustering mesh points in the boundary layer was used. In Figure 5, a 62×62 mesh generated over the flat plate is shown. The computational domain consists of a rectangle with length 0.5m and the height equals to five times of laminar boundary layer thickness.

As the initial condition (t=0), all quantities was set to their free stream values, which means that the plate is inserted suddenly into an undisturbed flow with free stream condition specified everywhere. The free stream Mach number was set to $M_\infty = 0.2$ for producing comparable results with incompressible flow equations and the Reynolds number was specified as $\mathrm{Re} = 1.2 \times 10^4$.

4 Results and Discussion

A flat plate has been considered as a test case to investigate the effects of Lorentz force in separation prevention at high angles of attack. The free stream angle of attacks was varied from 17 degrees up to 19.5 degrees. The electromagnetic field parameters were set according to the values tabulated in Table 1.

Computational results in form of density contours together with the domain vector plots are shown in Figure 6a for a flat plate at 18 degrees angle of attack. The closer view of these contours are shown in Figures 6b to 6e which indicate full separation over entire length of the flat plate as observed experimentally also shown in Figure 4a.

Similarly, computational results when applying Lorentz force in the form of density contours and the boundary layer vector plots are shown in Figure 7a for the flat plate at 18 degrees angle of attack. The closer view of these contours are shown in Figures 7b to 7e which show the entire boundary layer over the length of the flat plate is attached also observed experimentally in Figure 4b.

The lift coefficient was compared over a range of angle of attacks for "no Lorentz" and "with Lorentz" inclusion of the electromagnetic force in Figure 8. The maximum 0.8% lift rise was observed based on the values of electromagnetic parameters used at the angle of attack of 19.5 degrees. A slightly increase in drag coefficient can be observed at higher angles of attack due to increase in skin friction (see Figure 9).

The convergence history (RMS) of the numerical values of density was also shown in Figure 10. Convergence trends indicate two levels of drops of residuals after 5000 iterations.

5 Conclusions

The effects of Lorentz force in separation prevention for a flat plate at high angles of attack was studied numerically. To characterize the flow separation control, the arrangement of an experimental apparatus in a water channel was used for producing similar electromagnetic fields.

A class of high resolution TVD schemes was used for solving the compressible Navier-Stokes equations over the flat plate. The flat plate was computationally set to simulate low speeds at a range of angles of attack. In all cases studied, separation has completely prohibited using the Lorentz force induced by the electromagnetic field. By increasing angles of incidence, the lift coefficient as well as the drag coefficient over the plate has been increased. However, lift gain is greater than drag increase.

From this preliminary investigation, it is evident that the current CFD code can be used to accurately calculate flow fields in presence of electromagnetic fields and to examine it for a wide range of flow conditions. This concept may be used to increase performance of hydrofoils as well as airfoils at high speeds. This is the subject of current investigations where shock induced separation may be controlled for transonic and supersonic aircrafts.

References

1- Lüdwig Prantl, "Über Flüssigkeitsbewegung beisehr kleiner Reibung," In Verhandlg. III. Intern. Math. Kongr, p. 484-491, Heidelberg, 1904.
2- Gailitis, A. and Lielausis, O., "on a possibility to reduce the hydronamical resistance of a flat plate in an electrolyte," Applied Magnetohydrodynamic Reports of the Physic Institute, p. 12-143, 1961.
3- Nosenchuck, D.M. and Brown, G.L., "Direct spatial control of wall shear stress in a turbulent boundary layer," In so , R.M.C. , Speziale ,C.G. and Launder , B.E., editors, Near wall turbulent flows , p. 689-698, Elsevier, 1993.
4- Meng, J.C.S., Henoch, C.D, and Herbes, J.D., "Seawater electrohydrodynamics: A new frontier," Magnetohydrodynamics, 30(4), p. 401-418, 1994.
5- Henoch, C. and Stace, J., "Experimental investigation of salt water turbulent boundary layer modified by an applied streamwise

magnetohydrodynamic body force," Phys. Fluids, 7, p. 1371-1383,1995.
6- Crawford, C.H. and Karniadakis, G.E., " Reynolds stress analysis of EMHD-controlled wall turbulence. Part I. streamwise forcing," Phys. Fluid, 9, p. 788-806, 1997.
7- Nosenchuck, D.M., Brown, G.L., Culver,H.C., Eng, T.I. and Huang, I.S., " Spatial and temporal characteristics of boundary layers controlled with the Lorentz force," 12th Australian Fluid Mechanics Conference, p. 93-96, Sydney, 1995.
8- O'Sullivan, Peter L. and Biringen, Sedat, "Direct numerical simulations of low Reynolds number turbulent channel flow with EMHD control," Phys. Fluids, 10(5), p. 1181, 1998.
9- Grieberg, E., "On determination of properties of some potential fields," Applied Magnetohydrodynamics, Reports of the Physics Institute, 12, p. 147-154, 1961.
10- Weier, T., Fey, U., Gerbeth, G., Mutschke, G., and Avilov, V., "Boundary layer control by means of electromagnetic forces," ERCOFTAC Bulletin 44 2000 pp.36–40.
11- Tsinober, A.B. and Shtern, A.G., "On the possibility to increase the stability of the flow in the boundary layer by means of crossed electric and magnetic fields," Magnitnaya Gidrodinamica , 3(2), p. 152-154, 1967.
12- Weier, T., Gebeth ,G., Mutschke ,G. Platacicis, E., and Lialausis, o., "Experiments on cylinder wake stabilization in an electrolyte solutions by means of electromagnetic forces localized on the cylinder surface," Experimental Thermal and Fluid science, 16, p.84-91, 1998.
13- Yee, H. C. "Implicit Total Variation Diminishing (TVD) Schemes for Steady-State Calculations," J. Comp. Phys., 57, pp. 327-360, 1985.
14- Sedaghat, A., "A Finite Volume TVD Approach to Transonic Flow Computation" PHD Thesis, The University of Manchester, 1997.
15- Sedaghat, A., Shahpar S., Hall I.M., "Drag reduction for supercritical aerofoils", 20th ICAS Congress, Sorrento, Italy, 8-13 September 1996.

Table 1- Electromagnetic field parameters

L(m)	a(m)	$Re\times10^4$	j_0(A)	B_0(T)	α (deg)
0.5	0.01	1.24	10	1.0	18.0

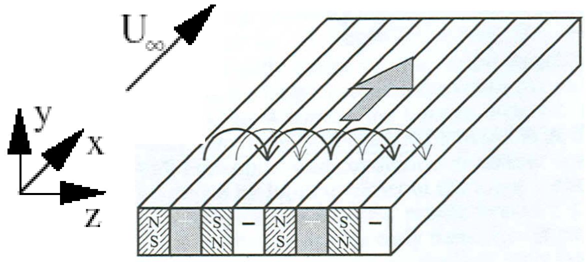

Fig. 1- Sketch of the electric (thin) and magnetic (thick) fields and the resulting Lorentz force (gray arrow) over a flat plate [10].

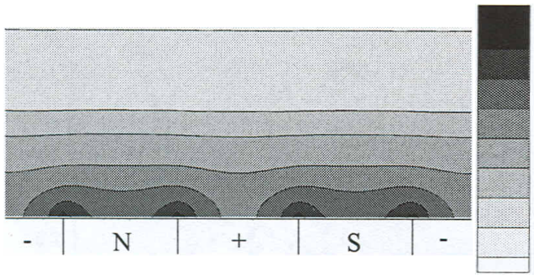

Fig. 2- Calculated Lorentz force distribution over the flat plate [10].

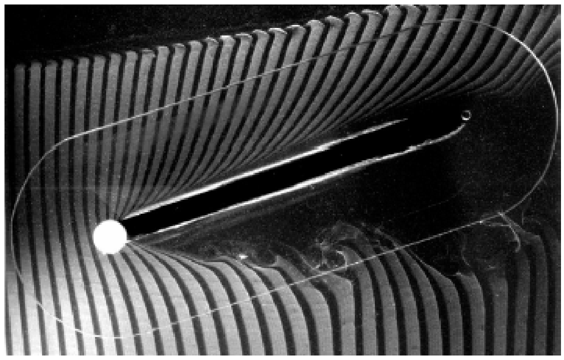

(a)

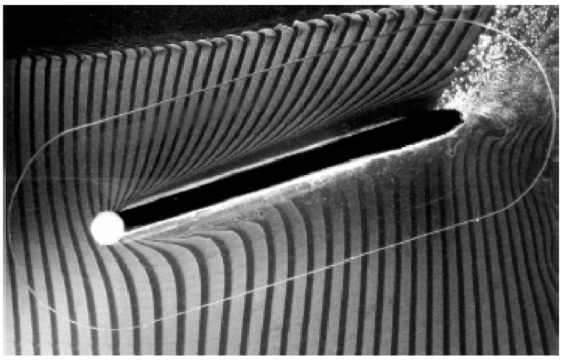

(b)

Fig. 3- Inclined plate without (a) and with (b) suction side Lorentz forces [10].

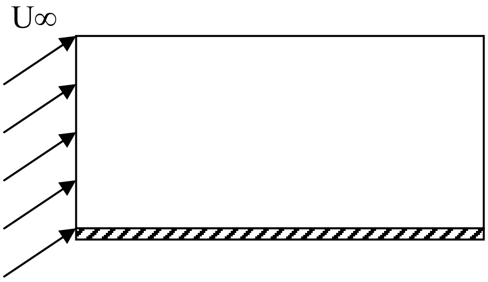

Fig. 4- The schematic of the problem for high incidence flow over a flat plate.

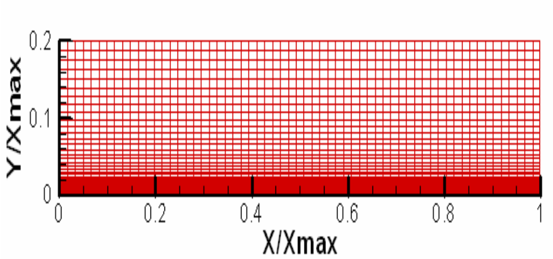

Fig. 5- The structured mesh generated for the computational domain over the flat plate.

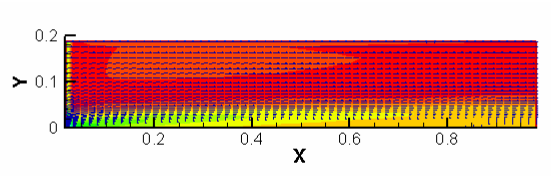

(a)

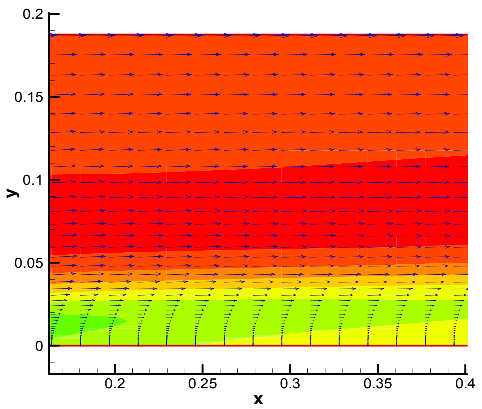

(b)

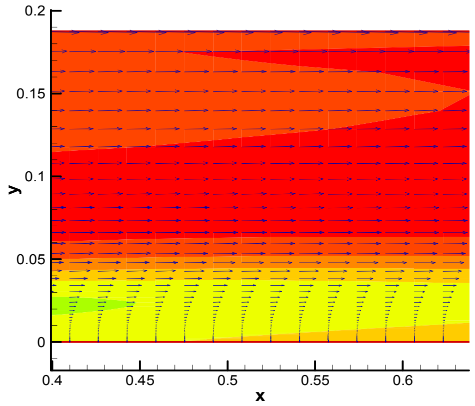

(c)

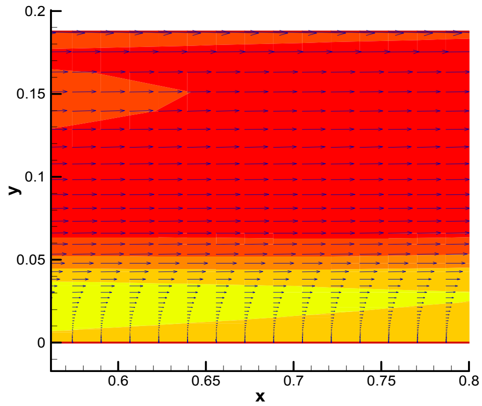

(d)

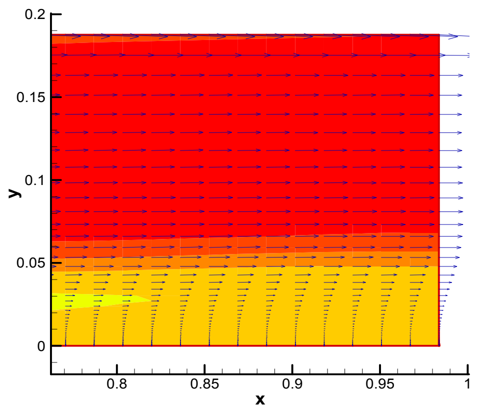

(e)

Fig. 6- Inclined plate without Lorentz force at $\alpha = 18^{\circ}, \mathrm{Re} = 1.4 \times 10^{4}$.

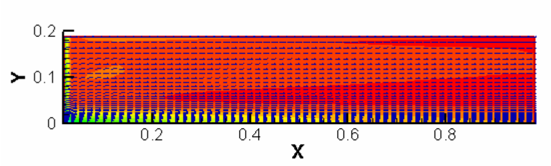

(a)

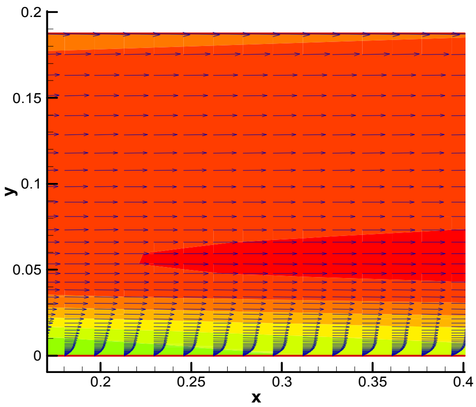

(b)

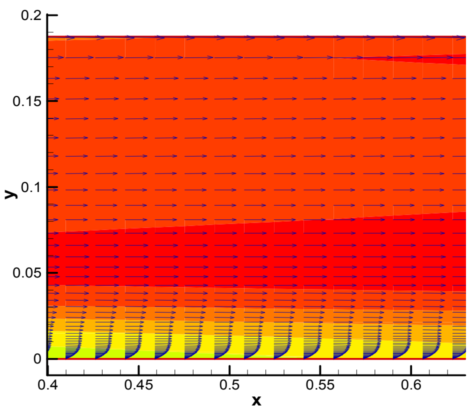

(c)

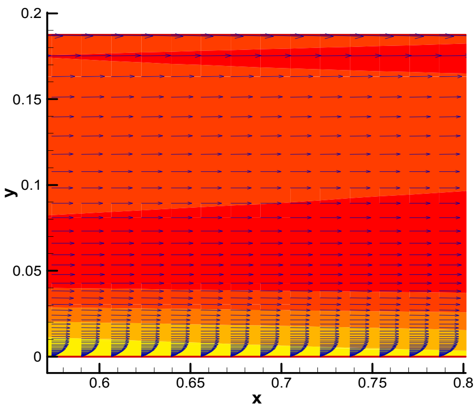

(d)

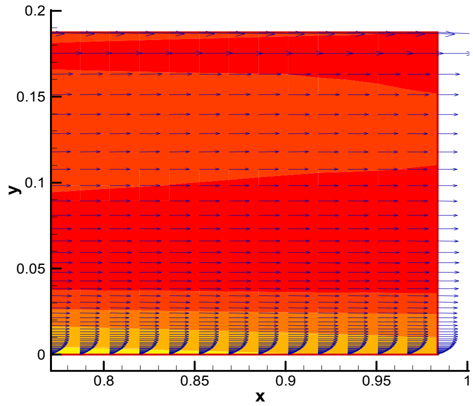

(e)

Fig. 7- Inclined plate with Lorentz force at $\alpha = 18^{\circ}$, $\mathrm{Re} = 1.4 \times 10^{4}$.

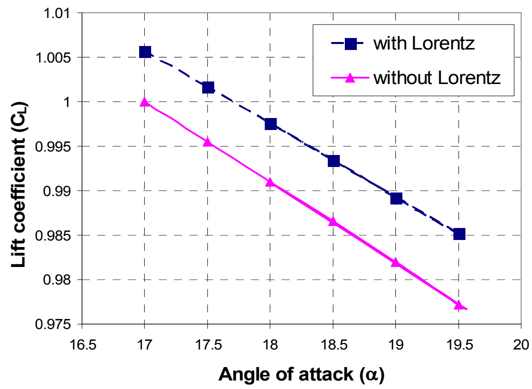

Fig. 8- Lift coefficient values for a flat plate showing effects of electromagnet field at $\mathrm{Re} = 1.4 \times 10^{4}$.

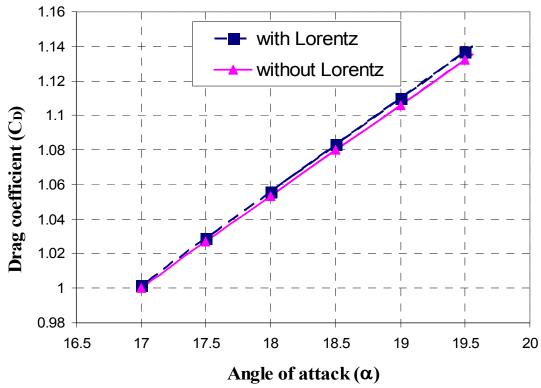

Fig. 9- Drag coefficient values for a flat plate showing effects of electromagnet field at $\mathrm{Re} = 1.4 \times 10^{4}$.

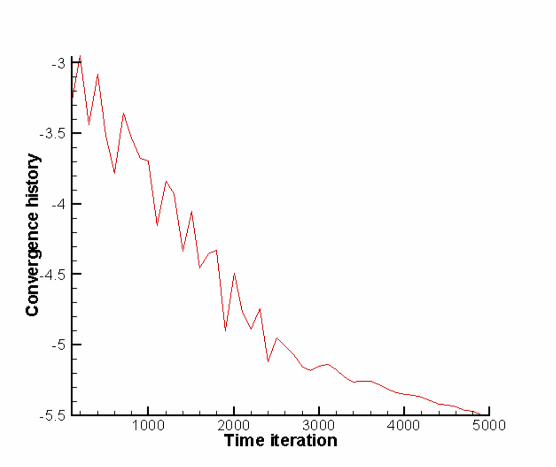

Fig. 10- Convergence history for density residuals.